Chapter 6

Studies on Cu/ZrO_2 surface composite fabricated by friction stir processing

As discussed in chapter 1, pure copper possessed superior thermal and electrical conductivity along with ease of fabrication (Barmouz et al., 2011a) and excellent resistance to oxidation and corrosion (Wang et al., 2017a) which make it a suitable material for several components in electrical, thermal, chemical, nuclear and transportation industries. However, poor wear resistance and low strength (Chen et al., 2018) and inferior arcing resistance limits its potential for application in electromechanical contacts, nozzles and bushes for bearings. Therefore researchers have been trying to enhance the hardness and the strength of copper through various processing techniques (Wang et al., 2018, Chen et al., 2018, Thankachan and Prakash, 2017). In this regard, particulate reinforcement in copper has gained the attention of researchers in recent years due to their excellent mechanical and wear properties along with ease of fabrication and low cost (Wang et al., 2009a, Koksal et al., 2012, Ramesh et al., 2009b). Ceramic particles such as TiC, Al2O3, Y2O3, and TiB2 possess high strength, elastic modulus and wear resistance and had been reinforced in the copper matrix to enhance its mechanical and wear properties (Wang et al., 2017b, Wang et al., 2016a, Chandrasekhar et al., 2014, Zhuo et al., 2013, Wang et al., 2015, Nalepka et al., 2016). Also, there are several challenges associated with the incorporation of ceramic particles in the copper matrix by melt based processes. For instance, the high temperature of melt causes the formation of some detrimental brittle phase at particle/matrix interfaces which leads to deterioration of mechanical properties (Bahrami et al., 2015, Bahrami et al., 2017). Also due to the density difference between matrix and particulates, particles tend to either float on the top or in the bottom. Further, it becomes very difficult to control aggregation and segregation of particles along grain boundaries which lead to decrease in strength (Suryanarayana and Al-Aqeeli, 2013). Aforementioned problems in the production of MMCs may be overcome by the application of solid state based processing techniques (Thankachan and Prakash, 2017, Schubert et al., 2008, Palanivel et al., 2016). To the best of our knowledge, there are no available reports on Cu/ZrO2 surface composite by FSP.

This chapter deals with the fabrication of Cu/ZrO2 surface composite via FSP. The performance of the fabricated composite has been assessed in terms of microstructural features, mechanical, tribological and electrical behaviour.

Chapter 6

Studies on Cu/ZrO_2 surface composite fabricated by friction stir processing

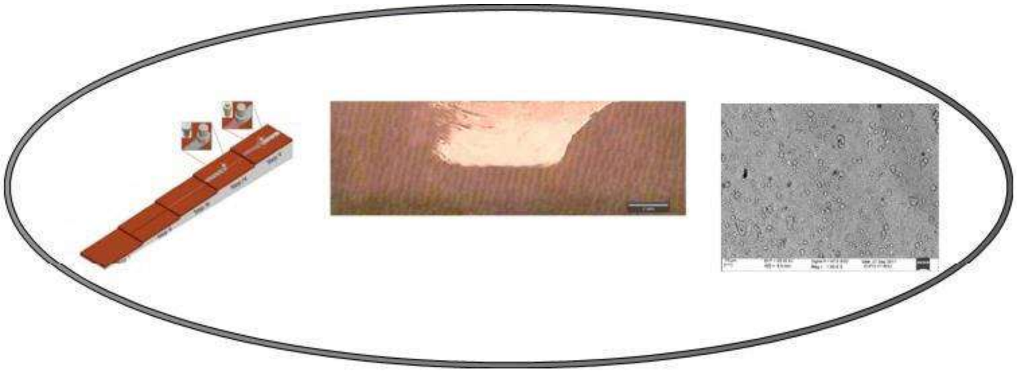

Results of this chapter have been published in

Kumar, H., Yusufzai, M.Z.K. and Vashista, M. ‘Microstructure, Mechanical and Electrical characterization of zirconia reinforced copper-based surface composite by friction stir process’, Material Research Express (2018) 5, 086505.

6.1 Introduction

This chapter reports studies on the fabrication of Cu/ZrO_2 surface composite by FSP and effect of zirconia reinforcement on microstructural features, mechanical, tribological and electrical behaviour. The microstructural evaluation was carried by optical microscopy, scanning electron microscopy and electron back scattered diffraction technique. Observed micrograph confirmed uniform dispersion of zirconia in the copper matrix. The stir zone (SZ) of the fabricated composite displayed equiaxed and fine grain structure. Compositional analysis of the composite was assessed through XRD. Mechanical properties of the composite were assessed by microhardness and tensile test. The hardness, wear resistance and tensile strength of the fabricated composite in SZ improved significantly as compared to as received copper. Grain size reduction and uniform dispersion of zirconia contributed to the improvement in hardness, wear resistance and tensile strength. The electrical conductivity of the fabricated composite was found to be less as compared to base copper. The post-assessment of the tensile specimen showed a reduction in ductility. The decreased electrical conductivity of the composite was ascribed to more scattering of electrons due to increased grain boundaries and non-conductive nature of zirconia.

6.2 Experimentation

6.2.1 Materials

The details of materials used for present investigation along with their chemical compositions are detailed in chapter 3 of section 3.2.

6.2.2 Fabrication of Cu/ZrO$_2$ composite

The procedure for the fabrication of Cu/ZrO$_2$ composite is detailed in chapter 3, section 3.3.

6.2.3 Characterisation of the composite

Characterization methods employed include optical microscopy, SEM, EBSD, XRD, microhardness, tensile testing, wear test and four-probe electrical conductivity measurement. The detailed procedures of all these characterizations are given in chapter 3, section 3.5.

6.3 Results and discussion

6.3.1 Macrostructure of the FSPed Cu/ZrO$_2$ composite

Fig. 6.1 depicts the macroscopic top view of fabricated Cu/ZrO$_2$ composite.

Figure 6. 1 The surface appearance of FSPed Cu/ZrO$_2$ surface composite

It clearly reveals the typical crown appearance having various ring-like patterns which is characteristics of FSPed plates. It can be also observed that the surface has no depressions or discontinuities. The clean crown appearance having no defects on the surface is the result of chosen processing parameters. If the processed surface has defects it will accompany the corresponding defects in the SZ of the fabricated composite. As the tool rotates and traverse, due to frictional heating copper plasticized and further get soften. This softens and plastically deformed copper flow from advancing side of the tool to retreating side of the tool. This flowing behaviour of the circle-form, softened band-layer per rotation of tool-shoulder led to the formation of surface ring-like textures.

The cross-sectional macrostructure of the fabricated Cu/ZrO_2 composite has been shown in Fig 6.2.

Figure 6. 2 The cross-sectional macrostructure of FSPed Cu/Zrconia surface composite

It is evident from Fig 6.2 that the macrostructure of fabricated Cu/ZrO_2 surface composite does not have any defects such as tunnels or pin holes. The stirring action of the rotating tool mixes the reinforced zirconia with severely plasticized copper and results into formation of Cu/ZrO_2 composite. The SZ of the composite resembles the basin-like shape i. e. the width of the top surface of SZ is wider than the width of the bottom of the SZ. The difference in width of the SZ at the top and bottom is believed to be due to material flow characteristics of the FSP process. Two types of material flow exist during FSP namely: shoulder driven and pin driven. At the certain depth of the SZ, the material flow during FSP is influenced by the shoulder, while below the certain depth it is driven by pin alone. Hence the width of the SZ decreases along the depth of SZ. The SZ in the present investigation is asymmetrical about the rotational axis of the tool. The reason for the asymmetry in the macrostructure of the SZ of the fabricated composite is supposed to be due to asymmetry in the material flow during FSP from advancing side to retreating side of the tool.

6.3.2 Microstructure of the FSPed Cu/ZrO_2 composite

Fig. 6.3 shows the optical micrograph of the fabricated Cu/zirconia surface composite at various locations within stir zone (SZ).

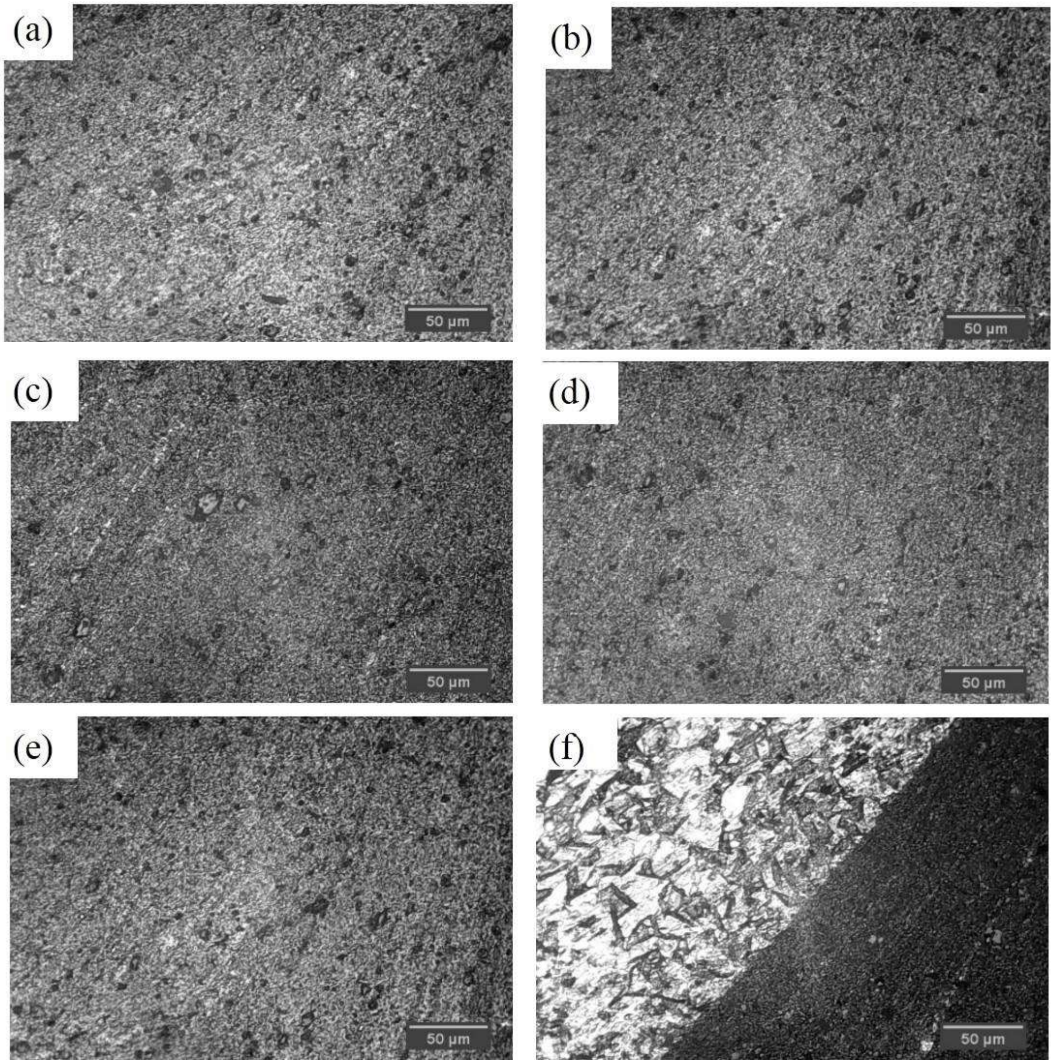

Figure 6. 3 Optical micrograph at various locations within SZ of the composite (a) towards advancing side at the top (b) towards retreating side on the top (a) at the centre towards advancing side (d) at the centre towards retreating side (e) towards advancing side at the bottom (f) Interface

It can be observed that the zirconia particles are spread all over the SZ of the fabricated composite. Furthermore, there is no concentration gradient of zirconia i. e. no variation in zirconia particle distribution is visible from advancing side to the retreating side or from the top side to the bottom side. Therefore, we can safely conclude that zirconia particle dispersion is almost constant throughout the stir zone under the investigated parameters. The insignificant concentration gradient of zirconia in SZ of the fabricated composite was attributed to sufficient plasticization of the copper matrix and solid-state nature of the FSP. Due to the higher viscosity of plasticized copper, zirconia particulates were not able to move freely in the copper matrix, so they could neither float on the top nor sink in the bottom which is generally observed in melt based processes. Thermally mechanically affected zone (TMAZ) and heat affected zone (HAZ) were missing as evident from the micrograph (Fig. 6.3(f)). The absence of TMAZ and HAZ can be attributed to higher heat transfer along the depth of the plate. It can also be observed that there was clear sign of formation of the banded structure of zirconia in the form of a concentric arc, generally termed as onion rings in SZ of the fabricated composite. This may be due to the higher temperature gradient along the depth of the plate which causes improper mixing of plasticized material in vertical and rotatory direction.

Fig. 6.4 shows the SEM micrographs of the fabricated composite at different magnifications.

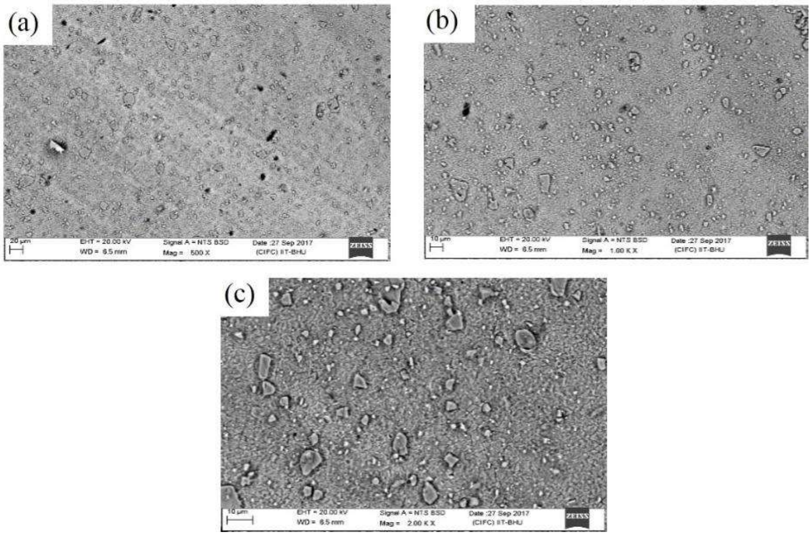

Figure 6. 4 SEM micrograph of SZ of the composite at different magnifications

The micrographs are an obvious witness of nature of dispersion and interface between the copper matrix and zirconia particulate. The entire region of the micrographs was occupied by reinforced zirconia particulate. Most of the particles are fairly equidistant from each other. No regions were found to be unreinforced and crowded with zirconia. So it can be concluded that zirconia dispersion was almost uniform in the copper matrix. This may be attributed to the proper selection of processing parameters. Due to sufficient stirring, packed zirconia mixed properly with plasticized copper matrix and resulted in uniformly dispersion of ZrO_2. Similar results have been reported by various researchers with uniform dispersion of particulates in the matrix by FSP (Thankachan and Prakash, 2017, Khorrami et al., 2015, Bauri et al., 2015, Narimani et al., 2016).

However, some contradictory results have also been reported (Mahmoud et al., 2008, Sahraeinejad et al., 2015, Sathiskumar et al., 2013) in which agglomeration within stir zone was observed. Fig. 6.4 (c) was taken at higher magnification to show the interface between copper and zirconia. It can be observed that the interface was continuous without any voids. The continuous interface may be attributed to smaller size and smooth surface of reinforced zirconia particles due to which plasticized copper flowed smoothly and adhered all over the zirconia particulate and thus resulted in the continuous interface. By comparing Fig. 3.2 (c) and Fig. 6.4 (c), it can be observed that there were no major changes in the shape and size of the reinforced zirconia particles after FSP. Various researchers have reported a change in the shape and size of reinforced ceramic particles during FSP (Sharma et al., 2015, Salih et al., 2015, Avettand-Fènoël and Simar, 2016). Metals deform plastically and can store energy in the form of elastic potential energy whereas, ceramics being brittle in nature, could not deform plastically and thus cannot store energy. Thus they undergo fragmentation during FSP. In the present investigation reinforced zirconia particles were smaller in size and have smooth surfaces so they did not provide much resistance to the flow of copper matrix and thus fragmentation did not happen. Moreover, the reinforced zirconia had no sharp corners, so stress could not concentrate over there and fragmentation did not occur. Fig. 6.5 depicts the EBSD images and particle size distribution of fabricated Cu/ZrO_2 composite.

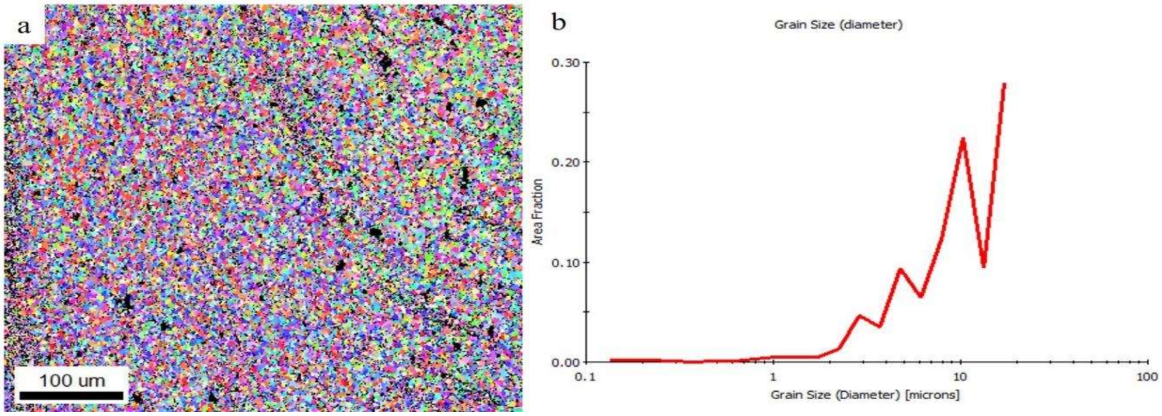

Figure 6. 5 (a) EBSD map and corresponding grain size distribution of particles (b)

The effect of FSP and zirconia reinforcement on grain structure is quite evident from the EBSD image. The grain structure of copper was coarse with a lot of twins (Fig. 3.1) as mentioned in section 3.2 of chapter 3. The estimated average grain size of base copper was 107 μm whereas it was 7 μm in case of the fabricated composite. The fabricated Cu/ZrO_2 composite has fine and equiaxed grain structure as compared to base copper. This drastic grain refinement in case of fabricated composite is attributed to dynamic recrystallization during FSP due to frictional heating and severe plastic deformation. Friction stir processing has a higher strain rate (up to 80 s^{-1}) (Mishra et al., 2003) which generates nucleating sites for new grains to grow and prevent grain growth. Also, uniformly dispersed zirconia pinned the motion of grain boundaries and slow down grain growth during dynamic recrystallization which led to grain refinement. Fig. 6.6 shows the XRD pattern of diffracted peaks corresponding to various phases present in the fabricated composite.

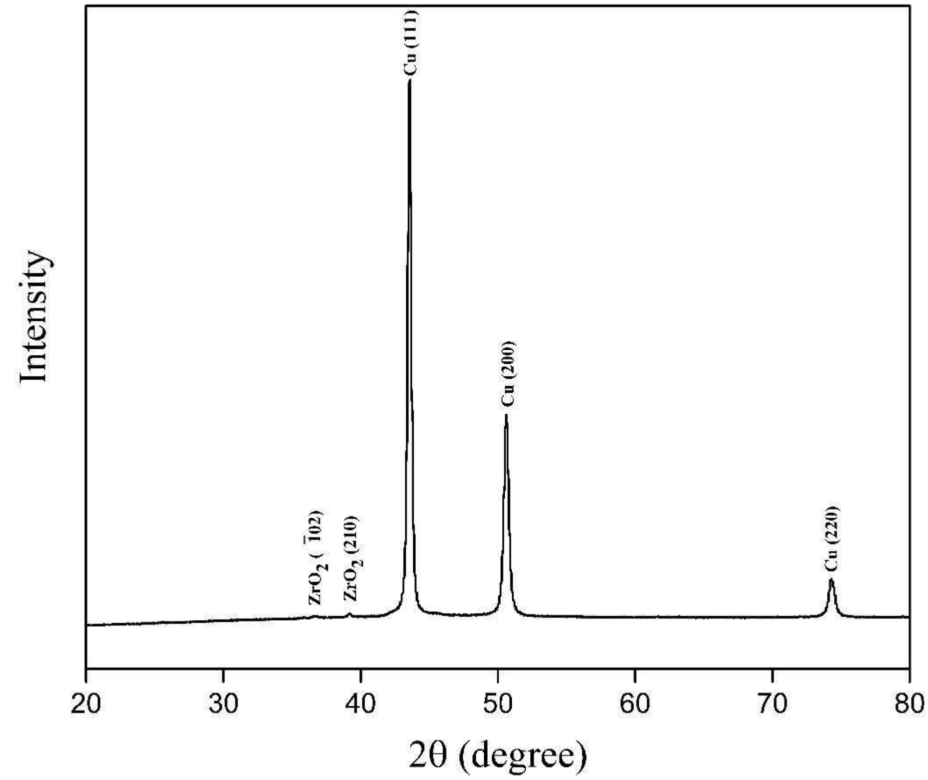

Figure 6. 6 XRD pattern of fabricated Cu/ ZrO_2 surface composite

It can be seen that diffraction peaks corresponding to ZrO_2 and copper are present in the XRD pattern. No diffraction peaks corresponding to any other phase that consists of both zirconia and copper were detected, that implied no occurrence of an in-situ reaction between zirconia and copper at an elevated temperature of FSP. This is mainly ascribed to the low reaction level between zirconia particulate and copper matrix caused by low processing temperature (0.8 Tm of copper (Dinaharan et al., 2017a)) and short thermal exposure duration of FSP.

6.3.3 Quantification of particle distribution of Cu/ ZrO$_2$ surface composite

The quantification of dispersion uniformity was done using the Lorenz Curve by considering the spatial location and area of each individual zirconia particle throughout the matrix. The image processing and data were acquired after binarizing the SEM image by ImageJ using quadrat method based on 20 equal sized quadrats having area 3161.95 µm^2 as shown in Fig. 6.7.

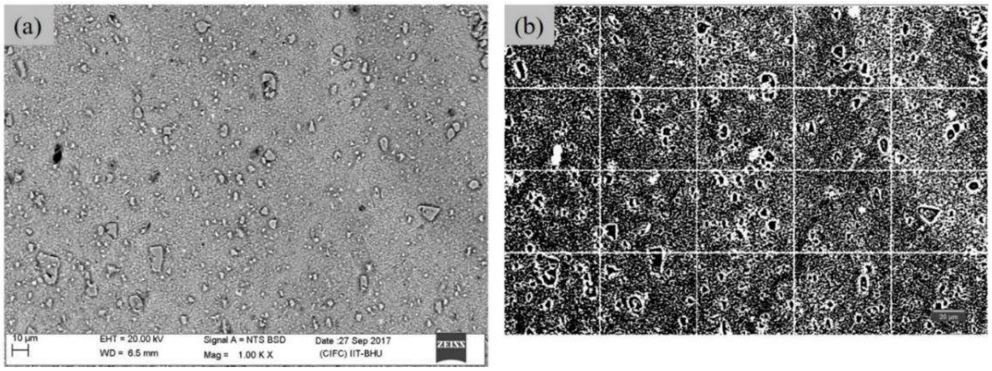

Figure 6. 7 SEM micrograph of fabricated composite Cu/ ZrO$_2$ and its binarized image (b). The dark spots are FA particles and white spots are a matrix

Also, the arithmetic mean of the area occupied by the zirconia particles in each quadrat was calculated. The quantification of the degree of distribution and homogeneity was obtained by evaluating the relation between an equality line and the Lorenz curve representing the partial homogeneity (Ceriani and Verme, 2012). The homogeneity was calculated using the following equation

$$H = 1 - G$$

Where H is homogeneity and G is Gini Index (Ceriani and Verme, 2012, Rossi et al., 2014). The Gini Index was chosen for the calculations since it was conceived as a measurement of the distribution inequality of a given attribute. Since the value of the ‘G’ is related to the area below the Lorentz curve (A_L) by G = 1- 2A_L, the homogeneity value is thus determined by H = 2A_L. The quantification of particle distribution was evaluated through Lorentz Curve is shown in Fig. 6.8.

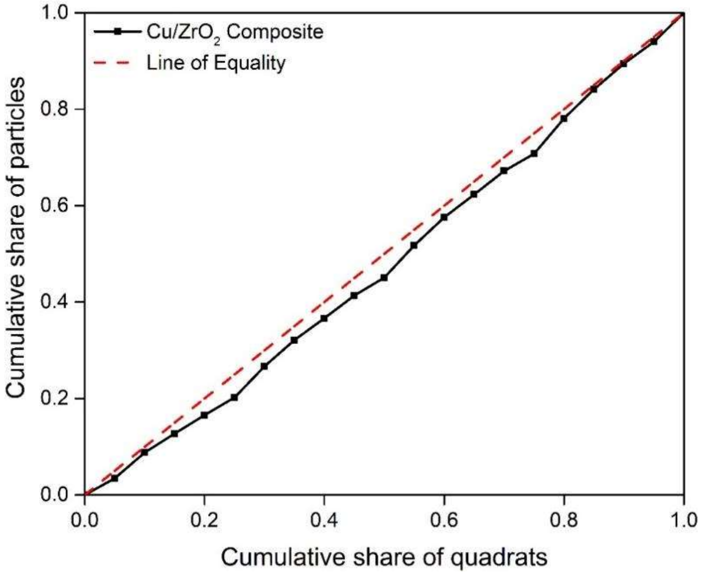

Figure 6. 8 Homogeneity curve for FA particles

From the Fig. 6.8, it is clear that the homogeneity curve for zirconia particles is very close to the Line of Equality. The calculated Gini Index and homogeneity value for the present case were found to be 0.051 and 94.8875% respectively. Which means zirconia particles were dispersed almost uniformly in the copper matrix and were almost equidistant from each other.

6.3.4 Mechanical properties

The mechanical properties assessment of base copper, FSPed copper without reinforcement and FSPed copper with reinforcement was adjudged through Vickers microhardness and tensile testing. The post-assessment of the tensile specimen was performed to find out the ductility. After tensile testing, the fractured samples were studied by SEM to have a detailed analysis of fractography.

6.3.4.1 Microhardness

Fig. 6.9. Shows the microhardness profile of the fabricated composite along the cross-section of SZ.

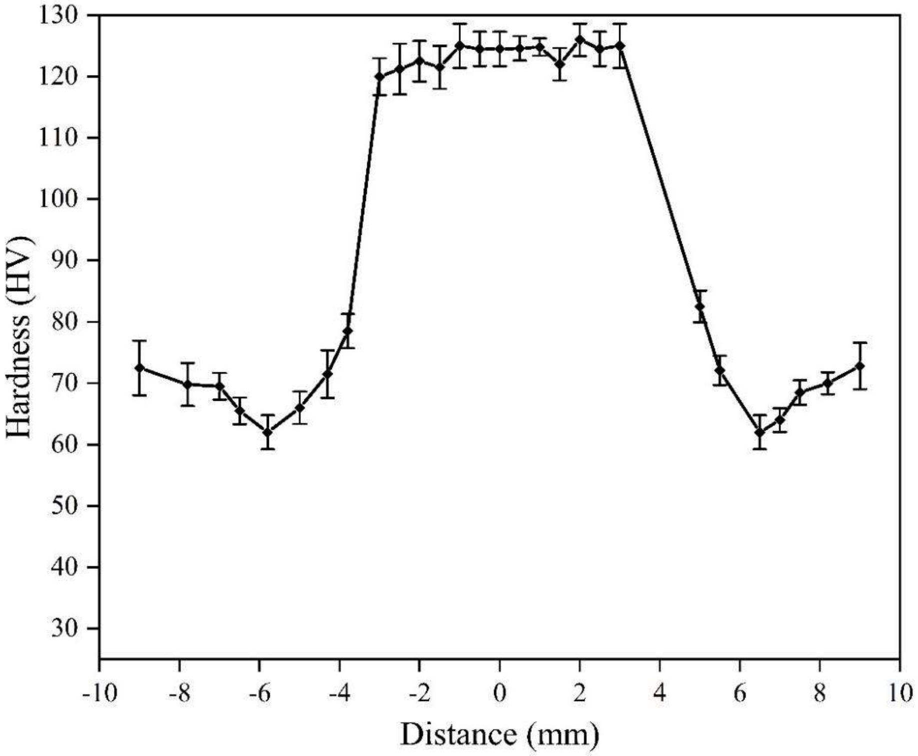

Figure 6. 9 Microhardness profile of FSPed Cu/ZrO_2 surface composite

It can be observed that the hardness in the side region of SZ has reduced slightly as compared to as received copper. Grain refinement and annealing effects may cause changes in the hardness of friction stir processed region during FSP. Due to dynamic recrystallization, the initial grains of base material changes to fine and equiaxed grains which led to an improvement in hardness according to the Hall Petch equation. Owing to annealing effects caused by a rise in temperature, dislocation density reduced and resulted in decreased hardness (Qu et al., 2011, Shafiei-Zarghani et al., 2011). Therefore, in the present investigation, the slight reduction in hardness in a side region of SZ is due to the dominance of annealing effects on grain refinement. From the microhardness profile, it can also be observed that zirconia reinforcement has improved hardness significantly in the SZ of the fabricated composite. The average microhardness value in SZ was estimated to be 123±4.8 HV i.e. 1.8 times higher than that of as received copper (67±3.6 HV). The improved hardness in the SZ may be attributed to the following strengthening effects. Firstly, the substantial grain refinement during FSP of composite led to improvement in hardness according to Hall-petch equation (grain refinement strengthening). Secondly, the uniformly dispersed zirconia particulates in the SZ of the fabricated composite provide a hindrance to dislocation movement due to the pinning effect (Orowan strengthening) (Zhang and Chen, 2008). Finally, the thermal mismatch (large difference in thermal coefficient) and different nature of deformation behaviour of copper and zirconia generated additional dislocations (Bauri et al., 2015) which piled up across grain boundaries and acted as a barrier to the free movement of dislocations (thermal expansion dislocation strengthening).

6.3.4.2 Tensile Properties

The stress-strain curve for the fabricated composite has been depicted in Fig. 6.10.

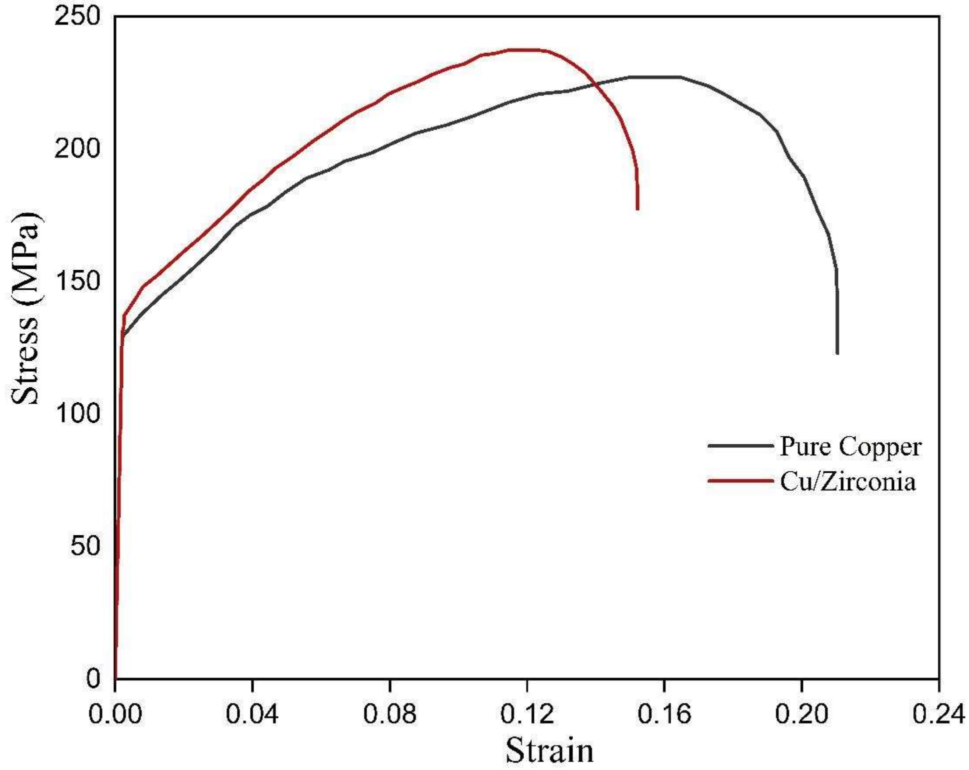

Figure 6. 10 Stress-strain curve of base copper FSPed Cu/ ZrO$_2$ surface composite

It can be seen that the strength of fabricated composite has improved as compared to base copper. The ultimate tensile and yield strength of fabricated composite was estimated to be 237±6.4 MPa and 131±5.8 MPa respectively whereas, it was 227±3.6 MPa and 129±4.1 MPa in case of commercially pure copper. The improvement in strength of the Cu/ZrO$_2$ composite is believed to be because of microstructural changes due to FSP and introduction of zirconia particles in the copper matrix. The possible strengthening factors are discussed below: The uniform and homogeneous distribution of zirconia particles in the copper matrix brings

Orowan mechanism into play during tensile loading. The composite experienced drastic grain refinement as compared to base copper and hence strength improvement occurs according to Hall-Petch relation. The difference in coefficient of thermal expansion of the base copper and reinforced zirconia particles generates additional dislocations which provide resistance to free movement of dislocations led to the higher strength of the composite. The percentage elongation in case of FSPed Cu/ZrO_2 composite has decreased with respect to base copper. The increased hardness and strength of composite may be the reason behind decreased ductility of composite. The reinforced zirconia particles resist the movement of dislocations by either creating stress field in the matrix or by inducing large differences in the elastic behaviour between the matrix and particulate (Barmouz et al., 2011a) and resulted in ductility reduction.

6.3.4.2.1 Fractography

Fig. 6.11 shows the fractured surface of the tensile tested Cu/ZrO_2 composite.

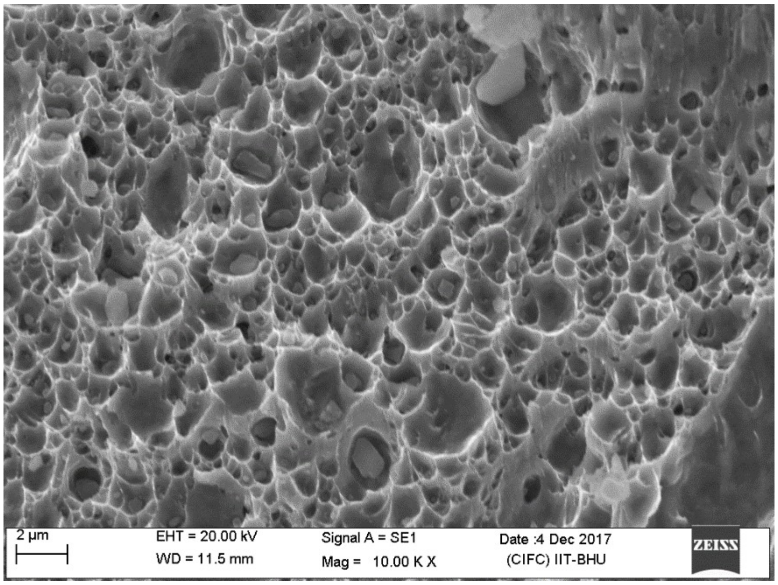

Figure 6. 11 Tensile fractograph of FSPed Cu/ZrO_2 surface composite

It can be observed that the dimples are narrow and shallow and flattened as compared to base copper (Fig.4.13a). This clearly implies that the ductility of the fabricated composite has decreased as compared to pure copper. This is in agreement with the result obtained analytically through stress-strain curve. The reinforced zirconia particles and FSP led to improvement in hardness and strength of the composite as mentioned earlier. The improved hardness and strength which lower their ability to plastically deformed and resulted into reduced ductility.

6.3.5 Tribological behaviour

Fig. 6.12 shows the variation of friction coefficient with respect to time for as received commercially pure copper and the Cu/ZrO$_2$ surface composite.

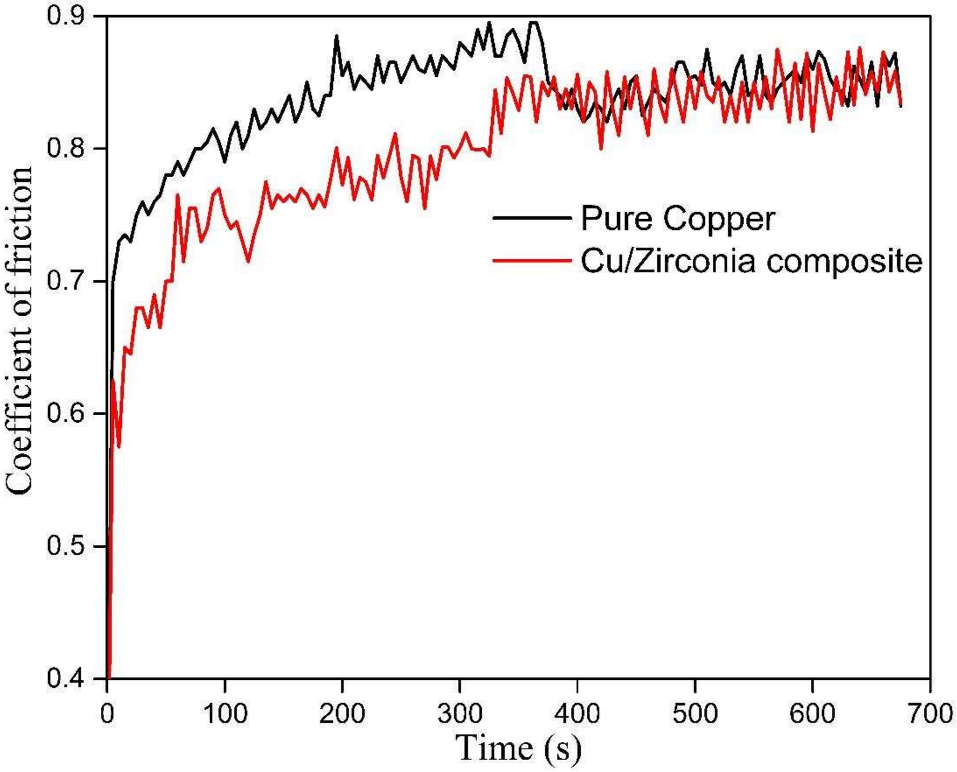

Figure 6. 12 Friction coefficient variation with time

It can be seen that the average value of friction coefficient in case of as received commercially pure copper is slightly less in comparison to Cu/ZrO_2 composite. It can also be observed that fluctuation in friction coefficient was slightly less in case of as received copper. Introduction of zirconia particles in as received copper led to an increase in abrasion resistance as the superficial hardness of the composite was more as compared to as received copper. So zirconia incorporation increased resistance to sliding and led increased friction coefficient. In case of as received copper, a thin tribo layer was formed on the surface of pin and counter body due to smearing of wear debris. However, it was prevented in case of composite due to the presence of zirconia particles and any layer formed was abraded by zirconia particles. Therefore, as received copper showed less fluctuation in friction coefficient as compared to Cu/ZrO_2 composite. Fig. 6.13 shows the results of wear test.

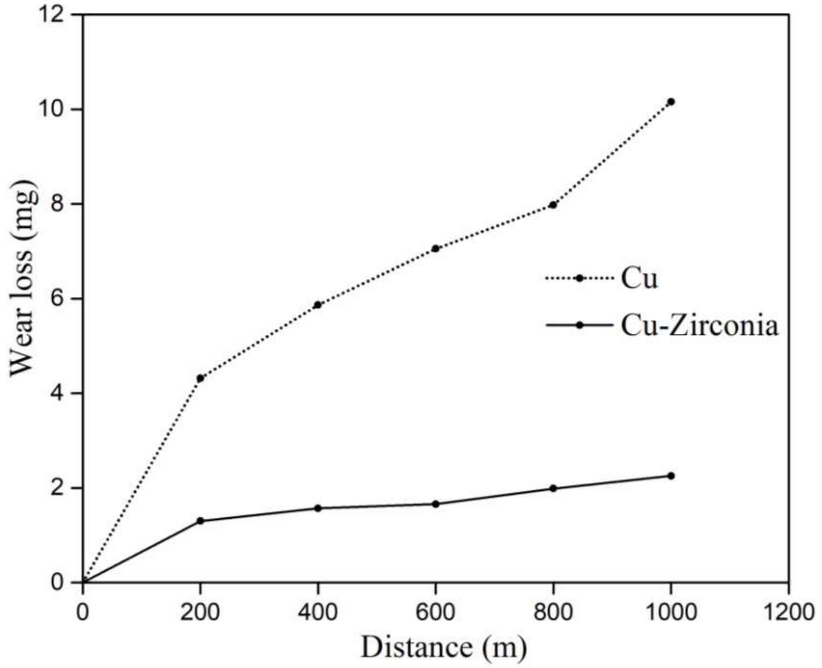

Figure 6. 13 Wear loss v/s distance profile of base copper and FSPed Cu/ZrO_2 composite

The weight loss in case of the fabricated composite (Cu/ZrO_2) was found to be less in comparison of as received copper. Fig. 6.14 (a) and (b) shows the SEM image of worn surfaces of as received copper and Cu/ZrO_2 composite respectively. Grooves due to ploughing effect can be observed in Fig. 6.14 (a). Delamination can also be seen in the micrograph (Fig. 6.14 (a)). Adhesion is dominant in case of as received copper in comparison of Cu/ZrO_2 composite. Adhesion caused delamination pits in as received copper. This led to severe material removal from the surface of copper. But in the case of Cu/Zirconia composite, the presence of hard Zirconia particles debilitated the effect of adhesion. Thus adhesive wear was very less in case of Cu/Zirconia composites as can be observed from Fig. 6.14 (b). The hardness of Cu/ZrO_2 composite was also higher as compared to as received copper which increased its resistance towards abrasive wear. The increase in abrasion resistance further reduces the wear loss of Cu/ZrO_2 composite.

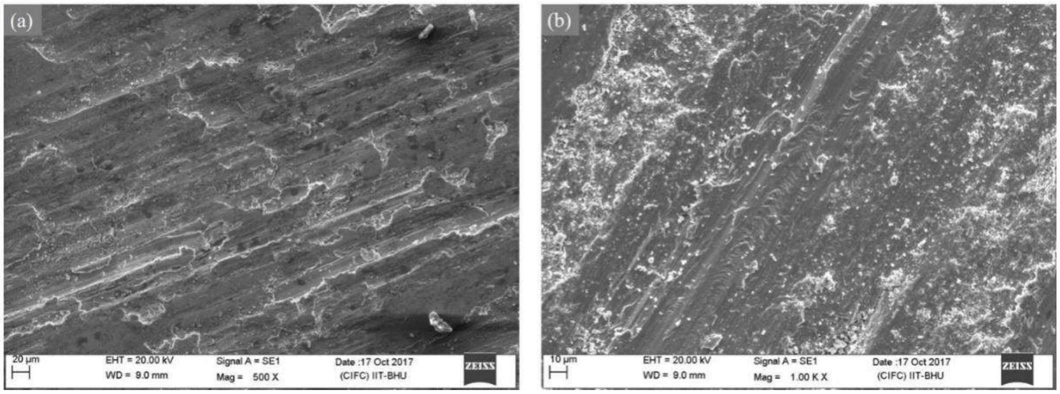

Figure 6. 14 SEM micrograph of the worn surface (a) Pure Copper (b) Fabricated Composite

6.3.6 Electrical conductivity

The electrical conductivity of Cu/ZrO_2 composite was estimated to be 69.64% IACS however it was 99.91% IACS in case of base copper. It can be seen that zirconia incorporation had adversely affected the electrical conductivity of the copper matrix. The decreased electrical conductivity of the fabricated Cu/ZrO_2 composite may be attributed to the scattering of electrons due to increased grain boundaries, impurities and non- conductive nature of zirconia. As mentioned earlier, zirconia reinforcement and FSP of Cu/ZrO_2 composite led to a drastic change in grain size of the copper matrix and thereby increased grain boundaries which affect the electrical conductivity of the composite. Further, the reinforced zirconia acted as impurities in the fabricated composite and increased the scattering sites for electrons and thus reduced electrical conductivity of the composite. The non- conductive nature of reinforced zirconia also contributed to the decreased electrical conductivity of the fabricated Cu/ZrO_2 composite.

6.4 Conclusions

Cu/ZrO_2 surface composite was successfully fabricated by the novel technique (i.e., FSP) and the effect of zirconia reinforcement on microstructural features, mechanical properties and electrical behaviour was studied in detail. The outcome of the investigation can be summarized as follows:

- Equiaxed and fine grain structure was observed in the fabricated composite as compared to base copper.
- The zirconia particulate was dispersed throughout the stir zone and the dispersion was almost uniform.
- Defects such as voids, pores, clustering and concentration gradient were not observed in SZ of the fabricated composite.
- The shape and size of reinforced zirconia did not change during FSP.

- XRD pattern of fabricated composite showed no peaks other than copper and zirconia.
- The microhardness of the fabricated composite was higher as compared to base copper.
- UTS and YS of the composite improved as compared to base copper and FSPed copper without reinforcement.
- The reinforcement of zirconia in the copper matrix had an adverse effect on the electrical conductivity and % EL of the fabricated composite.